Crystal symmetry and order-disorder structure of brewsterite

Mizuhiko Akizuki

Institute of Mineralogy, Petrology, and Economic Geology, Faculty of Science, Tohoku University, Sendai 980, Japan

Abstract

Brewsterite crystals from Strontian, Scotland, consist of various growth sectors such as $\{610\}$, $\{011\}$ and $\{0kl\}$, which correspond to the growth faces. The crystal symmetry, which is triclinic ($P1$) throughout the crystal, may be explained by Al-Si ordering that occurs on the crystal surface that is inclined to the mirror plane and twofold screw axis of pseudosymmetric space group $P2_1/m$.

Introduction

Brewsterite, a rare strontium zeolite, $Sr_2Al_4Si_{12}O_{32} \cdot 10H_2O$, was first found in Strontian, Scotland, by Brooke (1822). Des Cloizeaux (1874) observed brewsterite from Strontian between crossed polars and found that it was divided into three sectors visible in the (010) section. The crystal structure of brewsterite was determined in monoclinic space group $P2_1/m$ by Perrotta and Smith (1964) and refined in the same space group by Schlenker et al. (1977). The mineral, however, is piezoelectric (Ventriglia, 1953). The crystal elongation is parallel to the **a** axis in the structural setting currently in use (Perrotta and Smith, 1964; Khomyakov et al., 1970), although it had been assumed to be elongated along the **c** axis previously (Dana, 1892).

According to Damour (referred to in Dana, 1892, p. 577), when the brewsterite crystal was heated at 130°C in air, the crystal became opaque and pearly, and the loss of water was 7.7 wt%. The crystals became electrically charged and attracted one another while still hot. Gottardi and Galli (1985) showed the DTA curve, which has a shoulder at 50°C and three peaks at 190, 260, and 380°C.

On the basis of studies of the relationships between surface features and internal textures of many minerals, Akizuki (1981) and Akizuki and Konno (1985) interpreted their optical properties and internal textures as being produced by atomic ordering on side faces of the growth steps; furthermore, Akizuki suggested a general mechanism for formation of the growth sectors.

Observation

The monoclinic crystal form and faces of Strontian brewsterite are shown in Figure 1. The crystal is elongated along the **a** axis and has a perfect cleavage parallel to (010). The large crystal has some small brewsterite crystals growing on it in subparallel orientation. The (100) and (001) surfaces show striations parallel to (010), which are caused by alternating growth of the $f(610)$ and $(6\bar{1}0)$ crystal faces and the $k(011)$ and $(0\bar{1}1)$ faces, respectively. Figure 2 shows the $\{610\}$, $\{010\}$, and $\{011\}$ sectors in a thin section inclined slightly to (010). Small subparallel

crystals are observed both within the large crystal and on its surface. Figure 3 shows a schematic sketch of the growth sectors of brewsterite as they appear between crossed polars in a thin section cut normal to **a**.

The $\{610\}$ sector. In the section normal to the **a** axis, the $\{610\}$ sector shows optical extinction parallel to the (010) cleavage plane, and therefore the internal texture corresponding to the striations is not observed between crossed polars (Fig. 3). In a (001) thin section, however, the $\{610\}$ sector shows extinction inclined about 2°–3° to the **b** axis and polysynthetic $\{610\}$ and $\{6\bar{1}0\}$ reflection twins. Sections parallel to (100) and (001) do not show uniform extinction in the $\{610\}$ sector when rotated on the universal stage about the normal to (010). These observations suggest that the $\{610\}$ sector is triclinic.

The $\{010\}$ sector. Figure 4 shows an $\{010\}$ growth sector in the thin section cut normal to **a**. The (010) surface consists of $(0kl)$ and $(0k\bar{l})$ vicinal faces inclined to (010) and separated by a dihedral angle of ~1.4°. The $\{010\}$ sector therefore consists of intergrown $\{0kl\}$ and $\{0k\bar{l}\}$ sectors, with optical extinction directions symmetrically inclined ~0.5° to the (010) cleavage. Thin sections cut parallel to (100) and (001) do not show uniform extinction normal to the (010) cleavage during rotation around the monoclinic **b** axis on the universal stage. These observations suggest that the $\{010\}$ sector is triclinic.

The $\{011\}$ sector. Optical extinctions of the four $\{011\}$ sectors, as seen in the (100) thin section, are inclined to the **b** axis, but are related by the twin axis and twin plane
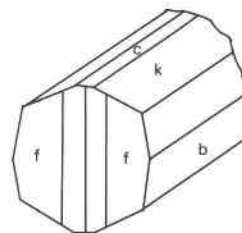

Fig. 1. Crystal form of brewsterite from Strontian, Scotland. The $b(010)$ face consists of two $(0kl)$ and $(0k\bar{l})$ vicinal faces.
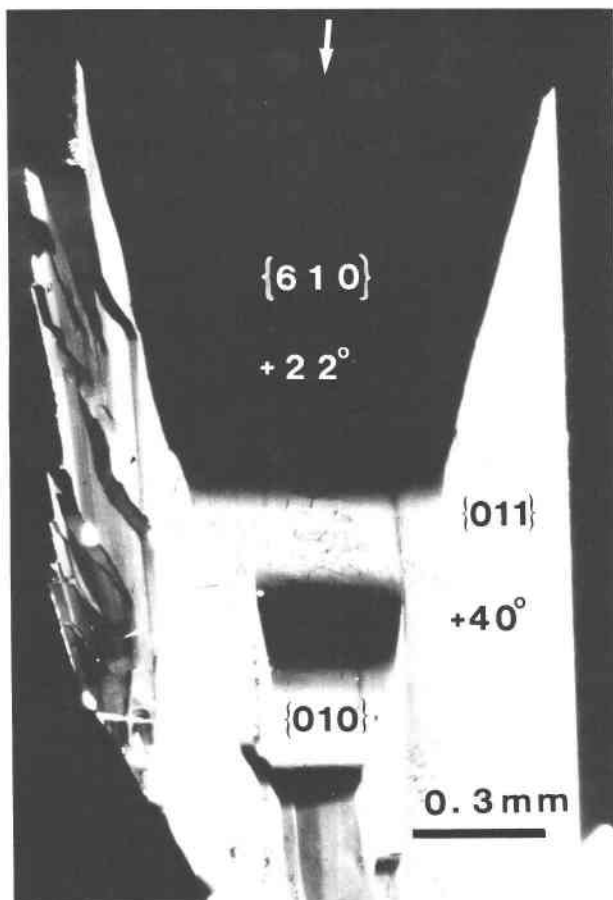
Fig. 2. Polarized photomicrograph showing sectoral zoning in a section of brewsterite inclined slightly to the (010). The arrow shows the crystal edge, which is not clear in the photograph. The crystal consists of the {610}, {011}, and {010} sectors, whose $2V$ values are indicated on the figure. The a axis is vertical. Crossed polars.
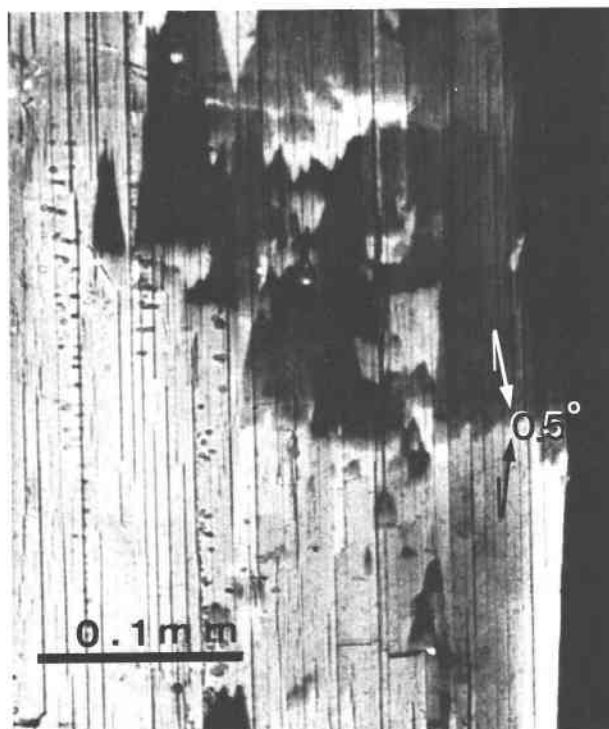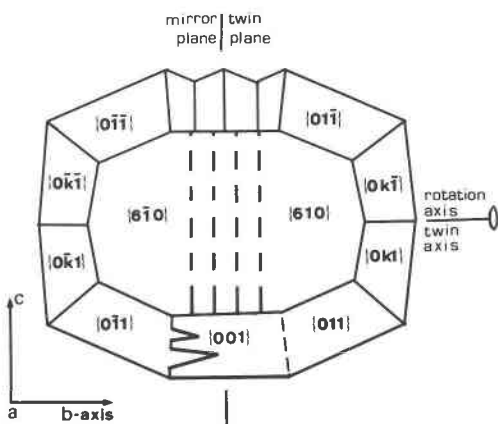

Fig. 3. Schematic sketch of the sectoral texture of a brewsterite crystal in the (100) section. Texture that corresponds to the striation on the (610) face is shown by dashed lines, because the texture is not observed in the (100) section. One of the (001) surfaces is flat, and another surface consists of a repetition of the (01Ī) and (0Ī1) faces, though actual crystals grow variously.

Fig. 4. Polarized photomicrograph showing the {010} sector in the (100) section of brewsterite. The (010) face consists of (0kl) and 0kĪ) vicinal faces. Extinction direction and angle from the (010) cleavage plane are indicated. The vertical lines are due to the (010) cleavage. Crossed polars.

shown in Figure 3. This suggests that the four {011} sectors are triclinic and comprise a fourling sectoral twin about **a**.

The {001} sector. The (001) face is flat, or striated with alternating (011) and (0Ī1) faces. The {001} sector with the flat (001) face is produced by intergrowth of the two kinds of domains that have extinctions similar to those of the {011} and {0Ī1} sectors. A similar kind of {001} sector consists of alternation of {011} and {0Ī1} slabs, corresponding to the surface feature. The symmetry here is triclinic, as well.

These observations suggest that brewsterite is triclinic throughout the volume of the crystal, although optical orientations and $2V$ values differ from sector to sector. Electron-microprobe analysis showed the crystal to be homogeneous, and X-ray diffraction peaks in the powder pattern were sharp, with no indication of peak splitting. After being heated at 200°C for 24 h, the thin section still showed triclinic symmetry, and the loss of water was 4.4 wt%. After heating at 250°C for 2 h, the specimen became opaque.

DISCUSSION

According to Perrotta and Smith (1964) and Schlenker et al. (1977), the Sr cation and three H_2O molecules (W_1, W_3, and W_4) are situated on the mirror plane in space
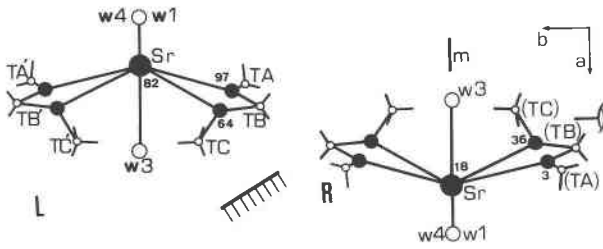
Fig. 5. Partial crystal structure of brewsterite projected on the **a-b** plane. The left (L) and right (R) figures are related by a twofold screw rotation. The crystal structure between the two figures (L and R) is omitted, because it is not directly coordinated to the Sr ion. The mirror plane (m) is vertical. Growth step on the (610) face is shown. The heights along the projection axis are shown as a percentage of the unit. Modified from Perrotta and Smith (1964).

group $P2_1/m$, and the four oxygens [two O(1) and two O(2) atoms] around Sr are bonded to the TA, TB, and TC sites (Fig. 6). The mean T–O distances indicate that TA, coordinated to an O(1) atom, contains 0.3Al; TC, coordinated to an O(2) atom, contains 0.4Al; and TB, which is bonded to both O(1) and O(2) atoms, contains 0.4Al. The TD site, however, which is not bonded to either O(1) or O(2) is occupied only by Si. The thin section shows that the crystal structure and texture were produced during crystal growth. This relationship suggests that Al-Si ordering can be attributed to charge-balance requirements between Sr and the T sites on the growth surfaces (Akizuki and Konno, 1985). Because Al-Si long-range ordering is incomplete, various short-range ordering schemes can be produced in brewsterite during crystal growth. The fact that triclinic symmetry was maintained after heating at 200°C may suggest that the symmetry is due to the tetrahedral ordering.

Figure 5 shows part of the crystal structure of brewsterite projected onto the (001) plane. The two parts of the figure (L and R) are related by a twofold screw rotation in the monoclinic space group $P2_1/m$, and the structure between the two parts, which is not directly coordinated to the Sr ion, is omitted. The (610) face is inclined to the monoclinic mirror plane and the twofold screw axis, reducing the symmetry in the {610} sector to triclinic (Akizuki and Konno, 1985). The TA tetrahedron is formed before the Sr atom enters the structure, whereas the TA' tetrahedron and Sr ion are on the steps simultaneously. This suggests that the TA site will be preferentially occupied by Si and that the TA' site will be preferentially occupied by Al in order to effect charge balance. If the crystal grows on the (6$\bar{1}$0) face, which is symmetrical to (610) with respect to the monoclinic mirror plane, a reverse relationship will occur among the T sites, resulting in twinning. TA and (TA) tetrahedra in Figure 5 are related topologically by the twofold screw axis and are thus topologically equivalent, but they are not equivalent with respect to the Sr ion on the growth step. Therefore, the Al-Si occupancy of the two tetrahedra is different, and the screw axis disappears. This reasoning suggests that the space group of the {610} sector is noncentrosymmetric, triclinic $P1$, and the mirror plane and the twofold screw axis of the monoclinic space group change into the twin plane and twin axis, respectively, consistent with the piezoelectric effect observed by Ventriglia (1953). Des Cloizeaux (1874) observed three sectors in the (010) thin section: a central wedge-shaped portion with sides that made angles of 17° and 13° with the front and back prismatic edges, respectively (see Dana, 1892, p. 577). The central portion corresponds to the {610} sector shown in Figure 3.
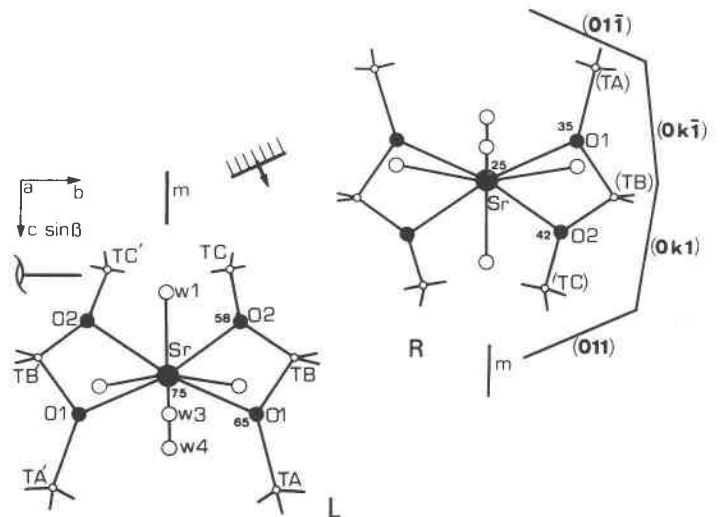
Figure 6 shows part of the crystal structure viewed down

Fig. 6. Partial crystal structure of brewsterite projected on the plane normal to the **a** axis. The two figures (L and R) are related as in Fig. 5. Growth step parallel to the (011) face is drawn. Crystal faces (011) and (0kl), which are normal to the paper, are represented. Modified from Perrotta and Smith (1964).

the **a** axis. Again, the L and R portions of the figure are related by the monoclinic screw axis, and the intervening part of the structure has been omitted. The (011) growth plane, which is inclined to both the mirror plane and the twofold screw axis, is shown. Although the TB and TB′ tetrahedra are equivalent in the three-dimensional structure, they are not equivalent on the growth step: the TB′ tetrahedron forms prior to filling of the Sr site during growth, whereas the TB tetrahedron forms after the Sr site is filled. Also, the TA and (TA) tetrahedra, which are related by the screw axis, are not equivalent with respect to the Sr cation on the (011) growth surface: the TA tetrahedron is added after the Sr ion on this surface, and the (TA) tetrahedron is added before the Sr ion. Similarly, neither the TB and (TB) tetrahedra, nor the TC and (TC) tetrahedra are equivalent. If these nonequivalences result in different relative preferences for Al and Si in the T sites, the four {011} sectors will also be noncentrosymmetric and triclinic, space group $P1$. Again, the morphological diad and mirror become a twin axis and twin plane, respectively, giving the {011} and {0$\bar{1}$1} sectors, and the {01$\bar{1}$} and {0$\bar{1}\bar{1}$} sectors a reflection-twin relationship. Furthermore, and two {011} and {01$\bar{1}$} sectors and the two {0$\bar{1}$1} and {0$\bar{1}\bar{1}$} sectors are related by a rotation-twin operation. The four triclinic {0k1} sectors, which are twin-related, are also produced by this mechanism. The triclinicity of brewsterite is too slight to be detected by X-ray diffraction, and no evidence of it has been found by neutron diffraction (Artioli et al., 1985).

REFERENCES

Akizuki, M. (1981) Origin of optical variation in analcime. American Mineralogist, 66, 403–409.

Akizuki, M., and Konno, H. (1985) Order-disorder structure and the internal texture of stilbite. American Mineralogist, 70, 814–821.

Artioli, G., Smith, J.V., and Kvic, Å. (1985) Multiple hydrogen positions in the zeolite brewsterite, $(Sr_{0.95}Ba_{0.05})Al_2Si_6O_{16} \cdot 5H_2O$. Acta Crystallographica, C41, 492–497.

Brooke, H.J. (1822) On the comptonite of Vesuvius, the brewsterite of Scotland, the stilbite and the heulandite. Edinburgh Philosophical Journal, 6, 112–115.

Dana, E.S. (1892) The system of mineralogy. Wiley, New York.

Des Cloizeaux, A. (1874) Manual de mineralogie, p. 420–422. Dunod, Editeur, Paris.

Gottardi, G., and Galli, E. (1985) Natural zeolites, minerals and rocks, 18. Springer-Verlag, Berlin.

Khomyakov, A.P., Katayeva, Z.T., Kurov, T.A., Rudnitskaya, Ye.S., and Smolyaninova, N.N. (1970) First find of brewsterite in the USSR (in Russian). Doklady Akademii Nauk S.S.S.R., 190, 1192–1195.

Perrotta, A.J., and Smith, J.V. (1964) The crystal structure of brewsterite. Acta Crystallographica, 17, 857–862.

Schlenker, J.L., Pluth, J.J., and Smith, J.V. (1977) Refinement of the crystal structure of brewsterite. Acta Crystallogrpahica, B33, 2907–2910.

Ventriglia, U. (1953) Simmetria della heulandite e piezoelecttricia di alcune zeoliti. Rendiconti della societá Italiana di Mineralogia e Petrologia, 9, 268–269.